Imaging flux avalanches in V_3Si superconducting thin films

Lincoln B. L. G. Pinheiro[1,2], Maycon Motta*[1], Fabiano Colauto[1], Tom H. Johansen[3], Emilio Bellingeri[4], Cristina Bernini[4], Carlo Ferdeghini[4], and Wilson A. Ortiz[1].

***Abstract*— When developing superconducting devices patterned on thin films one should bear in mind that flux avalanches might occur for some materials at a certain window of applied fields and temperatures. Although the A15 superconductors are well known and used in a variety of purposes, there are no studies about flux avalanches in V_3Si thin films. In the present work we report the observation of flux avalanches in films of V_3Si, grown by Pulsed Laser Deposition on a $LaAlO_3$ substrate. The range of temperatures and applied magnetic fields at which the avalanches take place was determined using dc-magnetometry. Magneto-Optical Imaging was employed to visualize the occurrence and spatial distribution of such flux avalanches. Images of the flux penetrated into the samples indicate a clear anisotropic distribution, which is ascribed to a thickness gradient. The observation of flux avalanches reported here imply that attention to this feature must be given when films of V_3Si are envisaged for possible applications.**

***Index-terms*: flux avalanches, V_3Si film, superconductivity, thickness gradient.**

I. INTRODUCTION

Promising improvements on superconducting devices such as nanowire single-photon detectors [1] and high-quality factor transmission line resonators [2] rely on a deeper understanding of vortex matter behavior, especially the vortex dynamics in thin films with which these devices are built. Although high compositional homogeneity and surface regularity are mandatory for these devices, thickness uniformity in thin films of superconducting materials is often limited to restricted regions of the substrate area, due to the geometric constraints of the film deposition process.

Local variations on the critical values of current and temperature (J_c and T_c) can lead to deformations on the penetrated flux distribution, and even to undesirable and abrupt events, in the form of flux avalanches. The origin of these avalanches is associated with the occurrence of thermomagnetic instabilities [3], which lead to the sudden invasion of magnetic flux rushing into the sample while leaving behind tracks of overheated material. Also known as flux jumps, avalanches in superconducting films constitute a rich and complex phenomenon which, however, might be detrimental to potential applications.

Although flux avalanches have been reported in single crystals of V_3Si [4], [5], [6], to the best of our knowledge, there was no direct observation of avalanches in thin films of this superconductor, whose class A15 includes materials of wide use in applications, such as Nb_3Ge and Nb_3Sn [7]. As a matter of fact, dendritic avalanches have already been observed in thin films of Nb_3Sn, as reported by Rudnev and coworkers [8]. In 1954 [9] a bulk sample of the compound V_3Si was for the first time reported to be a superconductor, with $T_c = 16.7$ K at ambient pressure [10], [11]. As a single crystal, it exhibits highly anisotropic critical current [12] and shows a low-temperature martensitic phase transition, from cubic at room temperature to tetragonal, below 30 K [13], [14]. This material also has interesting properties in the normal state, where it has been used in resistive switching memory devices [15], [16]. V_3Si has received attention recently due to the global interest in possible two-band superconductors - where ultra high-quality samples shaped as thin films are mandatory [17], [18], [19].

In this study we see - employing Magneto-Optical Imaging (MOI) - the distribution map of magnetic flux on the surface of thin films of V_3Si, a result that has not been reported so far in the literature.

II. MATERIAL AND METHODS

The V_3Si thin films were deposited on a (111)-oriented $LaAlO_3$ substrate by the PLD method, using stoichiometric targets in high vacuum. These films are polycrystalline and have the [210] crystallographic direction perpendicular to the substrate surface. At the center part of the substrate, the films are 180 nm thick. More details about the deposition parameters and characterization can be found in Ref. [17]. We used dc-magnetometry (DCM) in a Quantum Design MPMS-5S, to determine the magnetic phase diagram of the system. Magneto-Optical imaging was employed to visualize the spatial distribution of penetrated flux, as well as the occurrence and the morphology of flux avalanches (the experimental setup and further details about the MOI indicator are described elsewhere [20], [21], [22]). All MOI measurements were performed applying the magnetic field perpendicularly to the plane of the film, after a Zero Field Cooling (ZFC) procedure. Deviations from uniformity in the film thickness along its area were estimated by measuring the Si intensity peak all over the sample using a calibrated

* contact: m.motta@df.ufscar.br

[1]Departamento de Física, Universidade Federal de São Carlos, São Carlos, SP, Brazil.

[2]Instituto Federal de São Paulo, Campus São Carlos, 13565-905 São Carlos, SP, Brazil.

[3]Department of Physics, University of Oslo, POB 1048, Blindern, 0316 Oslo, Norway.

[4]CNR - SPIN, Corso Perrone 24, 16152 Genova, Italy.

Acknowledgments: This work was partially supported by the grants 2007/08072-0, 2017/24786-4, and 2018/16193-6 São Paulo Research Foundation (FAPESP), by the National Council for Scientific and Technological Development (CNPq), by the Coordenação de Aperfeiçoamento de Pessoal de Nível Superior - Brasil (CAPES) - Finance Code 001, by the Brazilian program Science without Borders, and by the Norwegian Research Council.

Energy Dispersive X-ray Spectrometry during Scanning Electron Microscopy measurements (EDS/SEM).

III. RESULTS AND DISCUSSION

Using AC magnetic susceptibility measurements (not shown) we found the critical temperature T_c of 14.5 $\pm$ 0.1 K and a broad normal-superconducting transition ($\delta T \approx 2$ K), at zero applied magnetic field. In order to investigate the instability regime, which is essential for applications, magnetization measurements were performed.

Fig.1 shows the DC magnetization as a function of the applied magnetic field, up to 100 Oe, in three different temperatures. Each of these curves is related to one of the MO images of Fig. 2. After a ZFC procedure, both the magnetization curves and the images were taken at constant temperature while the applied magnetic field was increased. The curve at 12 K shows a smooth behavior, indicating a critical-like penetration above H_{C1}.

The noisy response seen in the other two curves, at 2 K and 7 K respectively, are typical signatures of the occurrence of flux avalanches. The smaller fluctuations in the curve taken at 2 K can be directly related to what is seen in Fig. 2: smaller and less branched avalanches at lower temperatures. It is clear from Fig. 2 (b) that the avalanches from the upper border are longer and more numerous than those from the bottom, although both with few branches.

The larger jumps in the curve taken at 7 K in Fig. 1 reflect larger avalanches such as those shown in Fig. 2 (c). One can identify small avalanches in the low field regime close to all borders, ascribed to small jumps in the magnetic moment, at fields up to $\approx$ 30 Oe in Fig. 1. No avalanches were observed above the threshold temperature T* = 9.5 K. These measurements were repeated several times in order to verify the randomness of the branches - an import signature of this stochastic process related to thermomagnetic events - and such randomness was clearly observed. By repeating the experiment at higher temperatures, one can see fewer dendritic structures along with an increase in the degree of branching.

Fig. 3 shows a field versus temperature (HT) diagram compiled from magnetic measurements. The MO images taken in similar conditions of temperature and applied magnetic field, show the same behavior for the lower threshold. The upper threshold, however, could only be achieved by DCM. We placed in the diagram two different images of avalanches, triggered at the same field (23 Oe) and at the same position in the sample, but at different temperatures. One can easily observe that multiple ramifications of the avalanches are larger at higher temperatures. Such a diagram delineating the instability regime is likely to be helpful and should be consulted when designing devices for applications.

The panels (a) through (d) in Fig. 4 show Magneto-Optical images taken at 12 K, after a ZFC procedure, for fields - applied perpendicular to the plane of the film - up to 17.5 Oe. Dark and bright areas correspond here to low and high flux densities, respectively. The anisotropic shielding effect

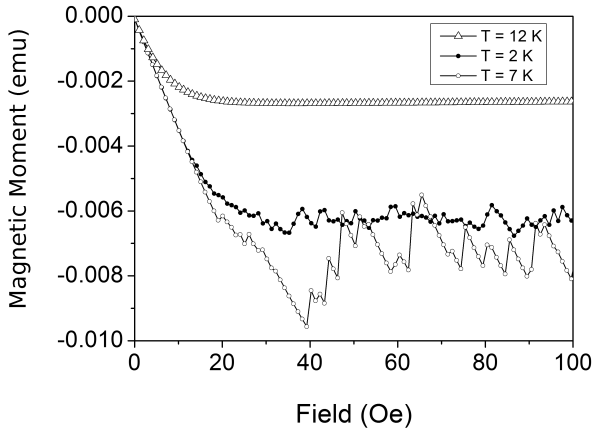

Fig. 1. Isothermal DC magnetization versus applied magnetic field taken at 2, 7 and 12 K, for a V_3Si film. For lower temperatures and H $>$ 10 Oe, the noisy behavior is the indicative of flux avalanches.

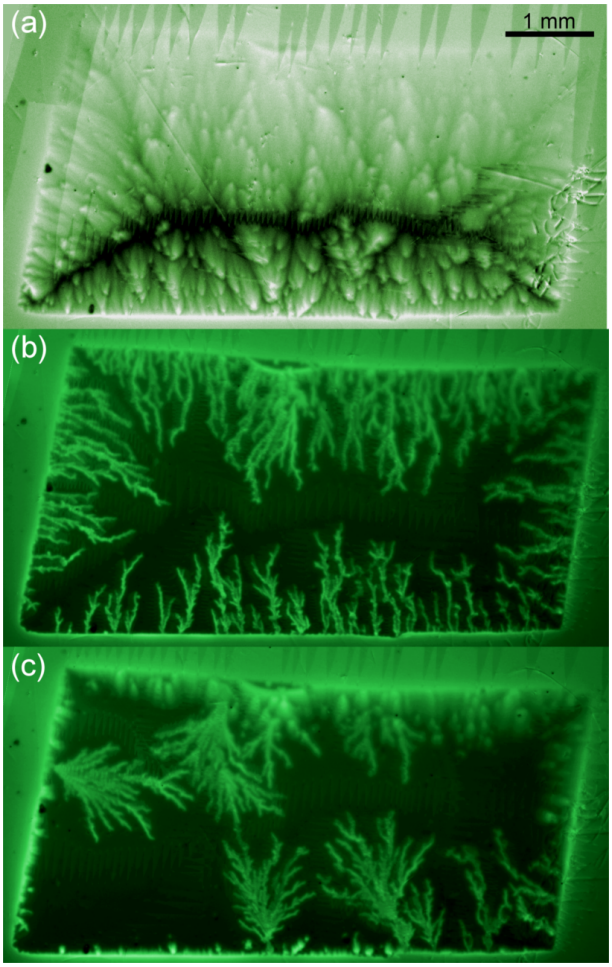

Fig. 2. Magneto-optical (MO) images taken after a ZFC procedure, applying H = 46 Oe: (a) full penetration of the flux at 12 K, where the granular character of the film can be clearly observed. (b) Flux jumps imprinted in V_3Si thin film at 2.47 K and (c) at 7.0 K.

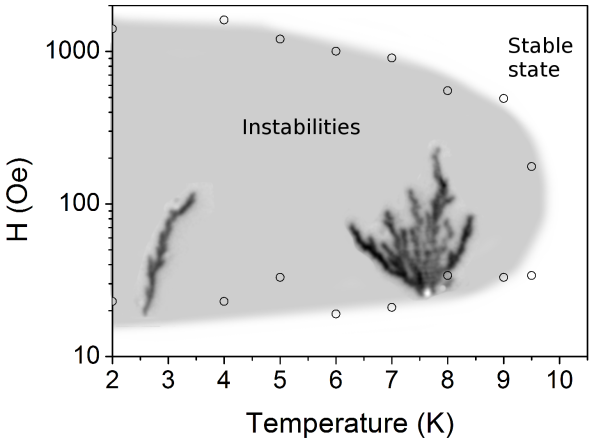

Fig. 3. HT diagram limiting the instability region, as determined by DCM measurements, in a V_3Si thin film while ramping up the field. Stability is recovered above a threshold temperature T* = 9,5 K. The avalanches, shown to illustrate the dendrict behavior, were both triggered for H = 23 Oe at 2.5 and 7.8 K respectively, and both have the same scale.

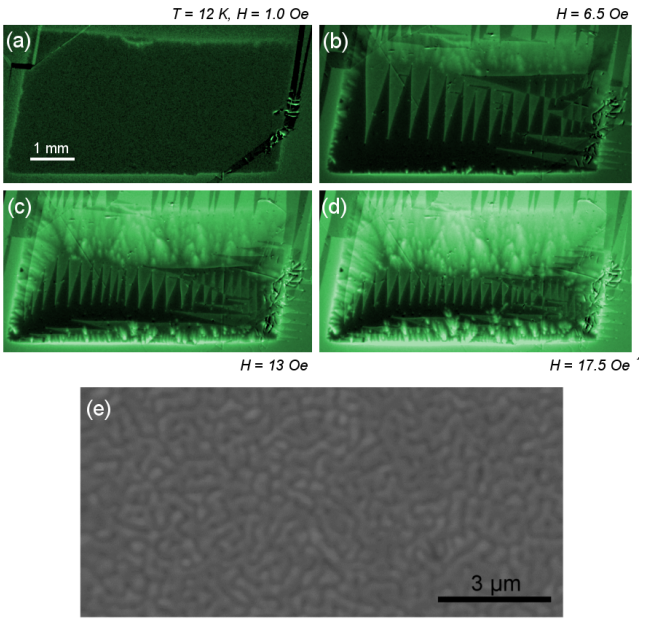

Fig. 4. Magneto-optical images of the smooth penetration into the V_3Si thin film at 12 K, taken in a slowly increasing field perpendicular to the plane of the sample: (a) H = 1.0 Oe; (b) H = 6.5 Oe; (c) H = 13.0 Oe and (d) H = 17.5 Oe. (e) SEM image of a sister sample, where the surface roughness shows granularity in the submicron scale.

is visible in Fig. 4, where the brightness level close to the sample edges shows an asymmetric decrease towards the center. The flux penetrates deeper into the sample from the upper and left edges, what is taken as an evidence of non-uniform thickness. In order to check this possible gradient in the thickness of the film, we made EDS measurements evaluating the intensity of the Si peaks. Mapping these peaks all across the sample we estimate an average thickness variation of 7 nm/mm along both directions parallel to the sample edges, which is consistent with the observed uneven flux penetration. However, another possible cause for the anisotropic shape of the penetrated flux front could be a temperature gradient across the film. Having in mind that the unidirectional heat removal from the cryostat cold finger could cause a temperature gradient across the film, we have reversed the sample, in order to check this possibility, which was ruled out by the experimental results.

The crystallographic orientation of the grains could also be thought as being the source of the anisotropy, since in a single crystal of V_3Si the ratio of the critical currents along different crystallographic directions can exceed 3 [12]. Nevertheless, this could only be the case for epitaxial thin films, not for the polycrystalline specimens studied here [17]. Figure 4 (e) shows a SEM image of a sister film, indicating granularity, as opposed to an epitaxially grown film. This granular character of the film is also manifested in MO images, as can be seen in panels (c) and (d) of Figure 4, which show that the penetrated flux exhibits a fanlike shape. This feature is known to reflect the existence of defects, either at the borders or within the film [23], [24], [25]. Evidences of a direct correlation between such flocking in the MO image and misorientations among grains has also been treated in Ref. [26].

IV. Conclusions

Flux avalanches of dendritic profile were observed, for the first time, in V_3Si thin films in the presence of a magnetic field applied perpendicularly to the plane of the film. Possible reasons for the anisotropic pattern of the penetrated flux front were investigated, leading to the conclusion that the cause is a non-negligible thickness gradient which, on average, amounts to 7 nm/mm. In view of this report of flux avalanches occurring in V_3Si, the list of superconducting films exhibiting this behavior is increased (see, e.g., [20] for a longer inventory) and, therefore, such a characteristic must be taken into consideration when films of this A15 superconductor are envisaged for possible applications.

References

[1] C. M. Natarajan, M. G. Tanner, and R. H. Hadfield *Superconductor Science and Technology*, vol. 25, no. 6, p. 063001, 2012.

[2] G. Hammer, S. Wuensch, M. Roesch, K. Ilin, E. Crocoll, and M. Siegel, "Coupling of Microwave Resonators to Feed Lines," *IEEE Transactions on Applied Superconductivity*, vol. 19, no. 3, pp. 565–569, 2009.

[3] R. G. Mints and A. L. Rakhmanov, "Critical state stability in type-II superconductors and superconducting-normal-metal composites," *Reviews of Modern Physics*, vol. 53, no. 3, pp. 551–592, 1981.

[4] G. Ravikumar, M. R. Singh, and H. Küpfer, "Measurement of magnetic relaxation in the peak regime of V3Si," *Physica C: Superconductivity and its Applications*, vol. 403, no. 1-2, pp. 25–31, 2004.

[5] A. Nabialek, V. Chabanenko, S. Vasiliev, G. Shushmakova, H. Szymczak, and B. Kodess, "Two components of the magnetostriction of the crystalline metallic V3Si superconductor," *Journal of Applied Physics*, vol. 105, no. 6, p. 063918, 2009.

[6] V. V. Chabanenko, B. N. Kodess, S. V. Vasiliev, A. Nabiałek, N. V. Kuzovoi, E. Kuchuk, S. A. Kononogov, and H. Szymczak, "Fine structure of thermal runaway process in the V3Si singlecrystal superconductor as a result of pinning center response," *Physics Procedia*, vol. 36, pp. 634–637, 2012.

[7] J. Muller, "A15-type superconductors," *Reports on Progress in Physics*, vol. 43, p. 48, 1980.
[8] I. Rudnev, S. Antonenko, D. Shantsev, T. Johansen, and A. Primenko, "Dendritic flux avalanches in superconducting nb3sn films," *Cryogenics*, vol. 43, no. 12, pp. 663 – 666, 2003.
[9] G. Hardy and J. Hulm, "The Superconductivity of Some Transition Metal Compounds," *Physical Review*, vol. 93, no. 1949, p. 1004, 1954.
[10] S. Tanaka, A. Miyake, B. Salce, D. Braithwaite, T. Kagayama, and K. Shimizu, "Pressure Investigation of Superconductivity of V_3Si," *Journal of Physics: Conference Series*, vol. 200, p. 012202, 2010.
[11] C. W. Chu and V. Diatschenko, "Study of Transforming and Nontransforming V3Si up to 29 kbar," *Physical Review Letters*, vol. 41, no. 8, pp. 572–575, 1978.
[12] M. Pulver, "Anisotropy of the critical data of superconducting V3Si-single crystals," *Zeitschrift fur Physik*, vol. 257, pp. 22–28, 1972.
[13] B. W. Batterman and C. S. Barrett, "Crystal Structure of Superconducting V_3Si," *Physical Review Letters*, vol. 13, no. 13, pp. 390–393, 1964.
[14] R. Brand and W. Webb, "Effects of stress and structure on critical current densities of superconducting V_3Si," *Solid State Communications*, vol. 7, pp. 19–21, 1969.
[15] D. Kim, D. Uk Lee, E. Kyu Kim, and W.-J. Cho, "Charge loss mechanism of non-volatile v3si nano-particles memory device," *Applied Physics Letters*, vol. 101, no. 23, 2012. cited By 4.
[16] D. Lee, D. Kim, K. Lee, and E. Kim, "Memory effect by carrier trapping into v3si nanocrystals among si02 layers on multi-layered graphene layer," *Journal of Nanoscience and Nanotechnology*, vol. 14, no. 11, pp. 8654–8658, 2014. cited By 0.
[17] C. Ferdeghini, E. Bellingeri, C. Fanciulli, M. Ferretti, P. Manfrinetti, I. Pallecchi, M. Putti, C. Tarantini, M. Tropeano, A. Andreone, G. Lamura, and R. Vaglio, "Superconducting Properties of V3Si Thin Films Grown by Pulsed Laser Ablation," *IEEE Transactions on Applied Superconductivity*, vol. 19, no. 3, pp. 2682–2685, 2009.
[18] M. Zehetmayer and J. Hecher, "Testing V_3Si for two-band superconductivity," *Superconductor Science and Technology*, vol. 27, no. 4, p. 6, 2014.
[19] P. K. Sinha and L. K. Mishra, "An Evaluation of Super Fluid Density as a Function of Reduced Temperature (T / T C) for Multi Gap Superconductors," *Journal of Pure Applied and Industrial Physics*, vol. 7, no. February, pp. 45–55, 2017.
[20] F. Colauto, M. Motta, A. Palau, M. G. Blamire, T. H. Johansen, and W. A. Ortiz, "First observation of flux avalanches in a-MoSi superconducting thin films," *IEEE Transactions on Applied Superconductivity*, vol. 25, no. 3, 2015.
[21] L. E. Helseth, R. W. Hansen, E. I. Il'yashenko, M. Baziljevich, and T. H. Johansen, "Faraday rotation spectra of bismuth-substituted ferrite garnet films with in-plane magnetization," *Phys. Rev. B*, vol. 64, p. 174406, Oct 2001.
[22] L. E. Helseth, A. G. Solovyev, R. W. Hansen, E. I. Il'yashenko, M. Baziljevich, and T. H. Johansen, "Faraday rotation and sensitivity of (100) bismuth-substituted ferrite garnet films," *Phys. Rev. B*, vol. 66, p. 064405, Aug 2002.
[23] J. Brisbois, O. A. Adami, J. I. Avila, M. Motta, W. A. Ortiz, N. D. Nguyen, P. Vanderbemden, B. Vanderheyden, R. B. G. Kramer, and A. V. Silhanek, "Magnetic flux penetration in Nb superconducting films with lithographically defined microindentations," *Physical Review B - Condensed Matter and Materials Physics*, vol. 93, no. 5, pp. 1–13, 2016.
[24] T. Schuster, M. Indenbom, M. Koblischka, H. Kuhn, and H. Kronmüller, "Observation of current-discontinuity lines in type-II superconductors," *Phys. Rev. B*, vol. 49, no. 5, pp. 3443–3452, 1994.
[25] M. Roussel, a. V. Pan, a. V. Bobyl, Y. Zhao, S. X. Dou, and T. H. Johansen, "Magnetic flux penetration in MgB 2 thin films produced by pulsed laser deposition," *Superconductor Science and Technology*, vol. 18, no. 10, pp. 1391–1395, 2005.
[26] A. E. Pashitski, A. Gurevich, A. A. Polyanskii, D. C. Larbalestier, A. Goyal, E. D. Specht, D. M. Kroeger, J. A. DeLuca, and J. E. Tkaczyk, "Reconstruction of Current Flow and Imaging of Current-Limiting Defects in Polycrystalline Superconducting Films," *Science (New York, N.Y.)*, vol. 275, no. 5298, pp. 367–9, 1997.